Article

Examining Spatiotemporal Photosynthetic Vegetation Trends in Djibouti Using Fractional Cover Metrics in the Digital Earth Africa Open Data Cube

Julee Wardle * and Zachary Phillips

Earth and Atmospheric Science Department, Saint Louis University, Saint Louis, MO 63103, USA;
zachary.phillips@slu.edu
* Correspondence: julee.wardle@slu.edu

Abstract: The Horn of Africa has sensitive, arid ecosystems, with its vegetation commonly distressed by factors such as climate change, population increase, unstable water resources, and rarely enforced land use management practices. These factors make countries such as Djibouti highly variable locations for the growth of vegetation and agricultural products, and these countries are becoming more vulnerable to food insecurity as the climate warms. The rapid growth of satellite and digital image processing technology over the last five decades has improved our ability to track long-term agricultural and vegetation changes. Data cubes are a newer approach to managing satellite imagery and studying temporal patterns. Here, we use the cloud-based Digital Earth Africa, Open Data Cube to analyze 30 years of Landsat imagery and orthomosaics. We analyze long-term trends in vegetation dynamics by comparing annual fractional cover metrics (photosynthetic vegetation, non-photosynthetic vegetation, and bare ground) to the Normalized Difference Vegetation Index. Investigating Djibouti-wide and regional vegetation trends, we provide a comparison of trends between districts and highlight a primary agricultural region in the southeast as a detailed example of vegetation change. The results of the Sen's slope and Mann–Kendall regression analyses of the data cube suggest a significant decline in vegetation ($p = 0.00002$), equating to a loss of ~0.09 km^2 of arable land per year (roughly 2.7 km^2 over the 30-year period). Overall, decreases in photosynthetic vegetation and increases in both non-photosynthetic vegetation and bare soil areas indicate that the region is becoming more arid and that land cover is responding to this trend.

Keywords: Open Data Cube; spatiotemporal trends; fractional cover; photosynthetic vegetation; Djibouti; food security; land cover trends

1. Introduction

Globally, vegetation in arid regions is often susceptible to the small shifts in temperature and precipitation that arise due to climate change [1–4]. Current research shows that arid regions are a challenging environment for vegetation to grow, and that agriculture and food security are closely tied to trends in climate change [5,6]. Global climate models predict increased variability in precipitation, higher temperatures, and more intense precipitation events [7]. These short-term variations drive the need for new analytical tools that can efficiently examine the long-term temporal trends of vegetation in response to climate change. The Digital Earth Africa (DEA) Open Data Cube (ODC) is a relatively new tool that efficiently addresses the existing problem of analyzing large quantities of remote sensing data for wide-ranging spatial scales across multiple decades.

The growth of satellite technology over the last five decades has improved the ability of scientists to track long-term vegetation change in arid regions where vegetation is sensitive to shifting climates. Satellite remote sensing is a leading technology in providing comprehensive information about numerous earth systems, particularly in monitoring global vegetation health and trends [8–14]. In handling remote sensing data, data cubes

are a newer approach to managing imagery, with hundreds or thousands of revisits to the same swath of land [15–17]. They are designed to efficiently store extensive sets of repeat imagery and are tailored for rapid access, processing, and analyses using a Python Application Programming Interface (API) [15,17,18]. The primary dimensions of a data cube for remote sensing purposes usually consist of the latitude, longitude, spectral data, and time [15]. The ODC is a non-profit, open-source data cube project driven by the need to uniformly manage and study temporally repetitive satellite data, and is freely available to the public [15–19].

DEA is an ODC initiative supported by the Australian Department of Foreign Affairs and Trade, funded in part by the Helmsley Charitable Trust and derived from Digital Earth Australia [20,21]. It maintains robust imagery libraries for the United States Geological Survey (USGS) Landsat mission, the European Commission (EC) and the European Space Agency (ESA) Copernicus Sentinel-2 mission. DEA also provides a cloud-based user computational platform in the form of a sandbox, operating in a Jupyter Notebook environment [20]. The ODC is freely available through DEA for users working on any type of African geospatial challenges [20–22].

The challenge being addressed here is analyzing the long-term temporal vegetation trends in arid Africa, with a focus on Djibouti. In the Horn of Africa, vegetation systems and agricultural areas are fragile ecosystems that are regularly distressed by extreme heat and drought, increasing populations, unstable water resources with limited irrigation options, and poor land use management practices such as a lack of crop rotation or a lack of controls for disease and pests [9,23–31]. Over half of the global population growth in the next 25 years is expected to occur in Africa. With this, the population of sub-Saharan Africa is projected to double by 2050 [8,32–34]. With future projections of climate warming and population growth, food systems and security will continue to be vulnerable in arid nations such as Djibouti [8,35–40].

Analyzing annual vegetation dynamics provides key information for determining the overall trends in natural vegetation and agricultural areas that may be subjected to abnormal drought, poor cropland management practices, or abandonment [41,42]. In arid regions, vegetation can be categorized either as photosynthetic (i.e., green leaves, healthy growing crops) or non-photosynthetic (dead/decaying/brown vegetation) [42–49]. Fractional cover algorithms use spectral unmixing [43,46–48] to determine the proportion of photosynthetic vegetation (pv), non-photosynthetic vegetation (npv), and bare soil (bs) (i.e., bare soil or rock) contained within a single pixel of imagery [44,46,49]. Comparing the ratios over months in a particular year and over multiple years indicates trends in a nation's land use management [47] and, more broadly, land cover.

This research (1) analyzed 30 years of Landsat fractional cover data products for Djibouti using DEA's ODC to quantify the fractional cover vegetation type (pv, npv, or bs), (2) compared the fractional cover results to the commonly used Normalized Difference Vegetation Index (NDVI) metric, and (3) tested for significant temporal trends using Mann–Kendall regressions and Sen's slope tests. For these statistical tests, we present a null hypothesis (H_0) of no trend in vegetation changes between 1990 and 2020, and an alternate hypothesis (H_a) of a significant trend in vegetation changes between 1990 and 2020. In the alternate hypothesis, the direction of the trend (positive or negative) is noted by the Mann–Kendall statistic and Sen's slope tests. For further clarification, in this study, the terms "photosynthetic cover" and "green cover" are used interchangeably to describe photosynthetic vegetation.

2. Materials and Methods

### 2.1. Area of Interest

Djibouti is a small country in the Horn of Africa (Figure 1), bordered by Eritrea to the north, Ethiopia to the west and south, and Somalia to the southeast. Djibouti has a population of approximately one million people and a land area of 23,200 km^2 [35,37,40,50–60]. However, only a small percentage of this land is considered cultivable due to factors such as aridity

and soil quality [52]. Only about 0.04% of Djibouti's land is classified as arable land, which is equivalent to around 9200 hectares or 92 square kilometers [40]. It receives an average of 147 mm/year of precipitation and had a water supply that could serve only half of the urban population and 21% of the rural population as of 1990 [40]. Its economy relies heavily on services, particularly those related to its status as a regional trade and logistics hub [52,53,61,62]. As a result, agriculture represents only a small fraction of its GDP, and it experiences frequent droughts that severely impact food security [50,51]. Djibouti is classified by the United Nations as a "chronic food-deficit country" due to its limited agricultural resources and recurrent droughts [40,52,53].
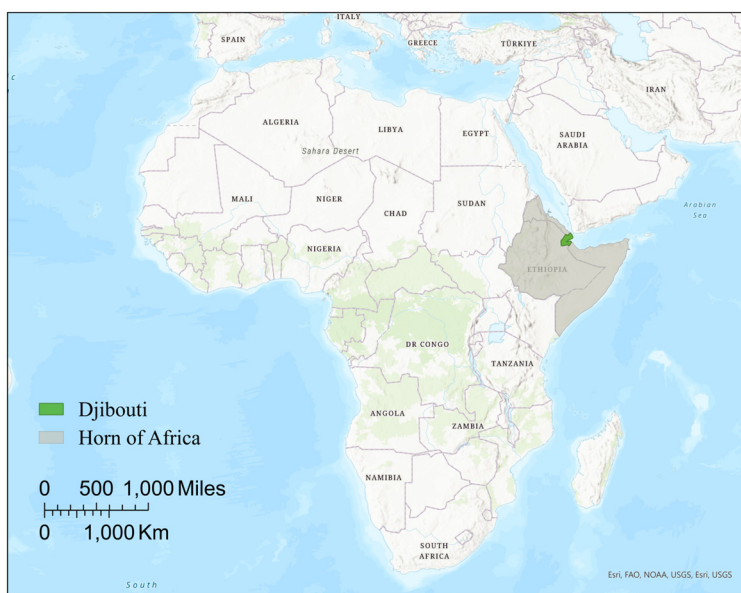
(A)
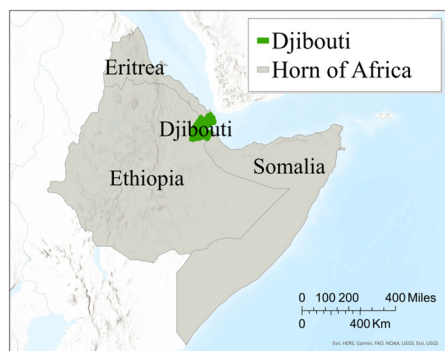
(B)
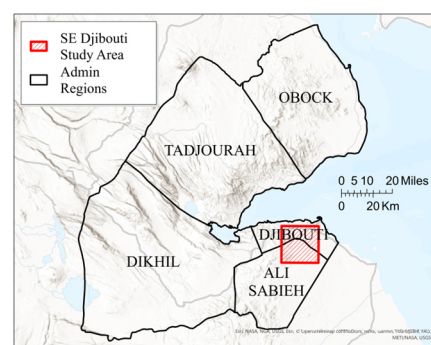
(C)

Figure 1. Location of Djibouti and study area in the arid Horn of Africa of the Eastern African Continent. Djibouti is one of ~20 African countries in arid regions. (**A**) Location of Djibouti and the Horn of Africa on the African Continent. (**B**) Djibouti location in the Horn of Africa. (**C**) SE Djibouti study area location and sub-regions in Djibouti.

For a more intent focus, a smaller, 23 km² study area (Figure 1C) was selected to exemplify the study results in raster format (Figure 2) and was selected in consultation with previous studies [63]. This smaller, exemplary region is the most visible cropland area in the region; it is prominently observable on satellite imagery and highlights an agriculturally important region in Djibouti District, just south of Djibouti City (Figure 1C). The region, while not inclusive of the entire country, served as a representation of the common regional geographic features and highlights one of the primary productive agricultural areas in

Djibouti. Agricultural production in Djibouti is concentrated in small pockets of fertile land located mainly in the southeast and northwest regions of the country [40,53].
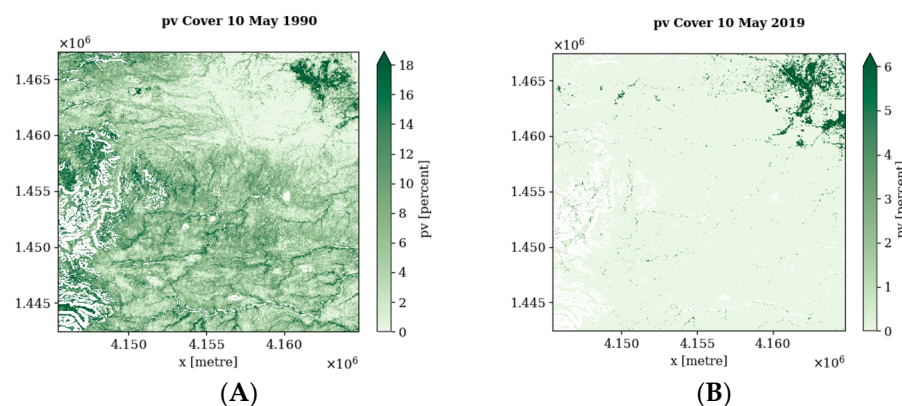

Figure 2. Example of photosynthetic vegetation (pv) cover in the SE Djibouti study area (Figure 1C) for the first and final portion of the 30-year period, May 1990 (**A**) and May 2019 (**B**).

2.2. Data Utilized

This study utilized several Landsat datasets, accessed for this study through the DEA platform. USGS Landsat Collection 2 Surface Reflectance imagery from Landsat 5, 7, 8, and 9 [20] was used by DEA to create the fractional cover (FC) products [41,64] for this study's 30-year study period (1990–2020). A Water Observations from Space product, also created by DEA [65], was used to mask the water and cloud pixels. An FC data cube was compiled using DEA's FC product to provide FC percentages at timesteps matching the Landsat satellite's 16-day temporal resolution. The FC products utilize each pixel in the study area at a 30 m cell size and use the WGS 1984 UTM Zone 38N Coordinate Reference System (CRS) (EPSG: 32638). Temporal data coverage is consistently available biweekly, aside from a two-year gap from 2006 to 2007 due to a Scan Line Corrector (SLC) failure with the Landsat 7 Enhanced Thematic Mapper plus (ETM+) sensor [66].

There are four bands in the FC dataset that express the percentage of fractional cover as an integer ranging between 0 and 100 for bare soil, photosynthetic (green) vegetation, and non-photosynthetic (dead/decaying) vegetation [12]. Also included is a fourth spectral unmixing error band [22] (Table 1).

Table 1. Data products and band IDs of fractional cover and water observations from space products derived from Landsat collection 2 surface reflectance.

Product	Description	Band ID	Name	Value Range	Units	No Data
fc_ls	Fractional Cover from Landsat	bs	bare soil	1–100	percent	255
		pv	photosynthetic vegetation	1–100	percent	255
		npv	non-photosynthetic vegetation	1–100	percent	255
		ue	unmixing error		1	255
wofs_ls	Water Observations from Space using Landsat	water	Water Observation Feature Layer	0–255	na	1

2.3. Processing in ODC

This study comprised three main processing phases: (1) computation structuring, (2) data compilation, and (3) analysis (Figure 3). We completed all three phases using DE Africa's online ODC python-based scripting environment. Parallel processing was used

to process the large volume of time slices in the data cube covering the thirty years and was accomplished using a four-core computer cluster and 28 gigabytes of memory. DEA utilizes Dask for dynamic task scheduling, which is a flexible library for parallel computing in Python [67]. It uses parallel arrays and data frames that run on top of dynamic task schedulers. Here, we assembled multiple data cubes to compare the FC and NDVI at both national and regional levels. A water and cloud mask were used to mask the presence of water and cloud pixels from the data cube, providing a cloud-free analysis.
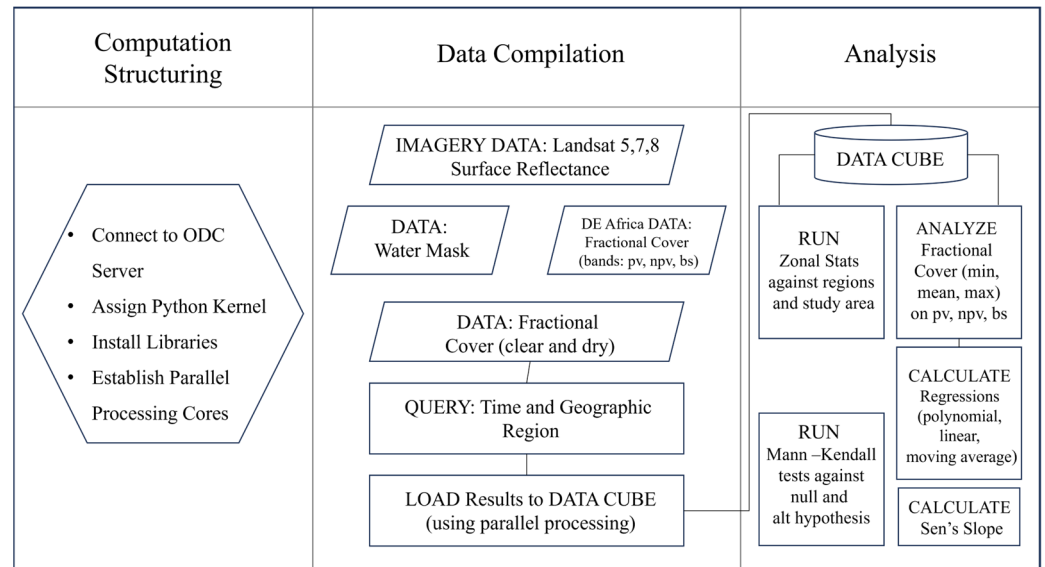
Figure 3. Methodology workflow encompassing the three processing phases of the study: computation structuring, data compilation, and analysis; these were all within the ODC environment.

2.4. Fractional Cover Calculations

The Joint Remote Sensing Research Program (JRSRP) developed the FC algorithms [41] used to build the DEA's bare soil (bs), photosynthetic vegetation (pv), and non-photosynthetic vegetation (npv) products, and DEA provided access to the algorithms and products as part of its analytic data sets [20]. The FC algorithm (Equation (1)), developed by Scarth et al. for Digital Earth Australia [41], is defined as

$$\begin{bmatrix} x \\ \delta \end{bmatrix} = \begin{bmatrix} M \\ \delta 1^T \end{bmatrix} f + e \qquad (1)$$

where δ is a weighting for the sum to one constraint and $1^T = \begin{bmatrix} 1 & 1 & \dots 1 \end{bmatrix}$ is a $c + 1$ vector of ones. The optimal value of δ is determined during the 10-fold cross validation process [41].

A comparison between the fractional cover and the more common NDVI provides insight into general relationships with a well-studied metric [42,44,45,47,49,68–70].

A spectral unmixing approach using the NDVI and the Cellulose Absorption Index (CAI) was applied in the creation of the FC product for this project [41,44,47]. In total, 675 images were filtered for clouds, leading to 119 scenes with less than 10% cloud cover being processed for the FC data products covering the period from 1 January 1990 to 1 January 2020. Each pixel in the Djibouti study area was input to the fractional cover algorithm after masking out cloud and water pixels.

We also conducted a district-level (Figure 1C) statistical comparison to summarize the changes over the 30-year period, including the minimum, maximum, range, mean, and standard deviation of pv values. The maximum values for pv signify the maximum cover level of green vegetation throughout the study period, the mean pv provides a general measure, and the minimum pv signifies the lowest level of green vegetation throughout the

study period. Variability/stability was measured using the range and standard deviation. Here, we present our results in the maximum, minimum, quartiles, and mean pv values by year. The maximum and minimum pv are the maximum or minimum pv value for any single pixel in any of the scenes contained within a given year, signifying both seasonal and spatial variations. The mean pv is the mean value in every pixel over the entire year. The presentation of results in this manner enables the average trends through the mean to be observed and highlights the locations and periods with the healthiest vegetation and most arid conditions.

Next, we summarized the FC results for each of the 119 scenes using the yearly FC maximum (wet season), minimum (dry season), and average to analyze consistent seasonal trends rather than include seasonal noise. We aggregated all scenes by year in the three categories (bs, pv, npv) for minimum, mean, and maximum levels, and calculated trendlines using linear and moving-average regressions for each.

2.5. Statistical Testing

Finally, the FC dataset was subjected to spatiotemporal statistical testing for photosynthetic vegetation, as photosynthetic vegetation is most frequently associated with healthy vegetation [47]. To test the direction of trends, we performed Sen's slope and Mann–Kendall trend tests (alpha = 0.05) to test the null (H_0) and alternate hypotheses (H_a):

- H_0: No significant temporal trend in FC types, by percent cover.
- H_a: Significant temporal trend in FC types, by percent cover.

Sen's slope and Mann–Kendall regressions are both methods of testing for trends in univariate, non-normally distributed temporal data. The direction of the trend (positive or negative) is noted by the Mann–Kendall (MK) test, where positive and negative values are, respectively, indicative of positive and negative temporal trends in photosynthetic vegetation over the entire 30-year study period. Mann–Kendall tests require computation of the z-statistic (Equation (2)), which is calculated as follows:

$$Z = (\tau - 1) / \left(\sqrt{Var(\tau)} \right) \tag{2}$$

where τ is Kendall's Tau, $Var(\tau)$ is the variance of Kendall's Tau, and Z is the test statistic. Kendall's Tau (Equation (3)) is the non-parametric correlation coefficient (or measure of association) for the sample and is defined as

$$\tau_n = \frac{c - d}{c + d} = \frac{S}{\binom{n}{2}} = \frac{2S}{n(n-1)} \tag{3}$$

where S is the number c of concordant pairs minus the number d of discordant pairs [71,72]. The Z-statistic is compared with the critical value to determine the significance of the trend in the time series data [71,73,74]. A significant result indicates the presence of a trend, either positive or negative, while a non-significant result suggests the absence of a significant trend [71,74].

Sen's slope was then used to provide an estimate of the 95% confidence interval around the mean trend. The Sen's slope test is a non-parametric method used to estimate the slope or trend in a time series by computing the median of all possible slopes between pairs of data points. It is robust to outliers and does not assume any specific distribution of the data. The calculation contains two steps:

1. For each pair of data points (x_i, x_j) in the time series, calculate the slope as $(x_j - x_i)/(j - i)$, where i and j are the indices of the data points.
2. Compute the median of all calculated slopes. This median slope is considered the Sen's slope [73,75–77].

3. Results

3.1. Fractional Cover Regression

Analysis of the temporal trends in total green vegetation showed both periods of increase and decrease over the thirty-year period, but the overall pv fractional cover decreased between 1990 and 2020 with a −0.00025 slope (Figure 4). Non-photosynthetic vegetation and bare soil comprised 35–60% of the study area, and photosynthetic vegetation accounted for only 10% of the fractional cover (Figure 4). The non-photosynthetic vegetation and bare soil had negative correlations with photosynthetic vegetation, and both displayed increasing trends over the study period. Each point on the graph (Figure 4) represents the average value for pv, npv, and bs for each of the 119 images in the data cube.
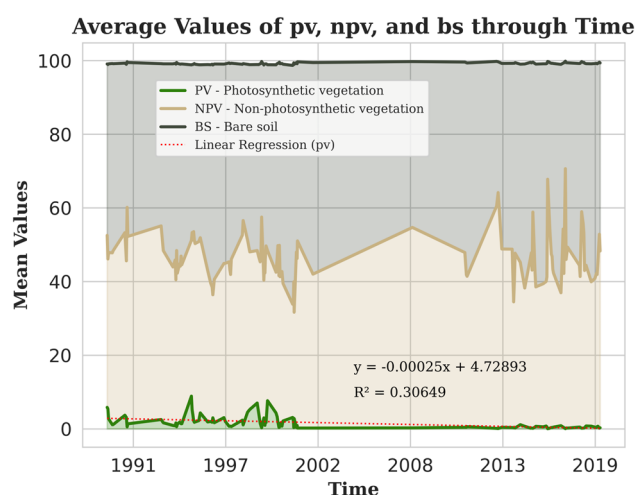

Figure 4. Image-averaged FC values (in percent) of the study area for the 30-year study period (119 cloud-free scenes total). The pv (photosynthetic vegetation) makes up less than 10% of cover annually and shows an overall decrease, whereas npv and bs show high variability and a slight increase throughout the study period.

The change in photosynthetic (green) vegetation for all 119 scenes of the study area showed a clear decreasing trend in the linear average (Figure 4). The linear regression slope was −0.00025 per year and showed a weak association with the input data (R^2 = 0.30649). Considering the area of Djibouti (23,200 km²), this means that Djibouti has lost the equivalent of 5.8 hectares of pv per year, which equates to 174 hectares over the 30-year study period.

To account for seasonal variability, we aggregated the pv data to the yearly level, reducing the time cube from 119 images (Figure 5A) to 30 annual composites, one for each year, and re-analyzed the regressions (Figure 5B–D). The decreasing trend in green vegetation was more readily observable when the data were aggregated annually to show the mean (Figure 5B), minimum (Figure 5C), and maximum (Figure 5D) photosynthetic vegetation levels for each of the 30 years.

The aggregated mean pv regressions showed similar results to the pre-aggregated dataset with a regression coefficient of −0.00028 and an R-squared of 0.73902 (Figure 5B). The aggregated minimum pv showed a slightly lower regression coefficient of −0.00011 and an R-square of 0.67484 (Figure 5C). The maximum green FC showed a linear regression coefficient of −0.00051 and an R-squared of 0.61761 (Figure 5D). The mean, min and max regression values represent various stages of photosynthetic vegetative growth, whether early spring-like growth (min) or full peak-season growth (max).
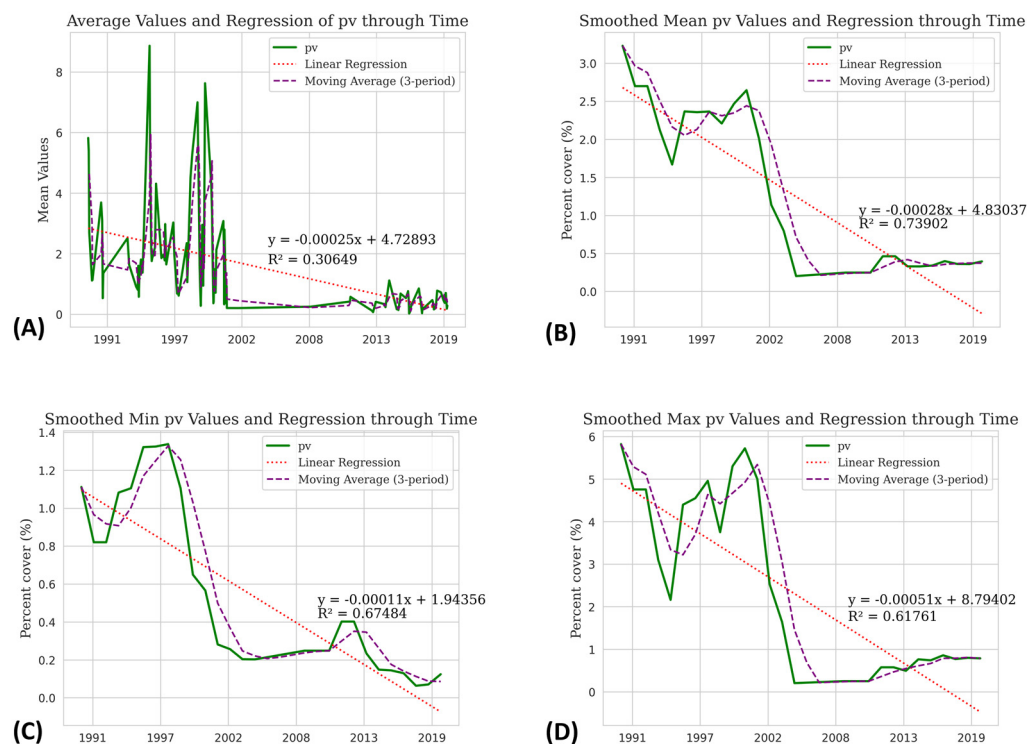
Figure 5. Summary trends of pv, 30-year linear trend, and three-year averages for all imagery in SE Djibouti study area (Figure 1C) (**A**); annual mean composite pv, 30-year linear trend, and three-year averages for mean pv (**B**); annual minimum composite pv, 30-year linear trend, and three-year averages for mean pv (**C**); and annual maximum composite pv, 30-year linear trend, and three-year averages for mean pv (**D**).

3.2. Mann–Kendall and Sen's Slope Tests

All trends show general decreases in green fractional cover throughout the 30 years. The Mann–Kendall test (Table 2) rejected the null hypothesis (H_0 = no change in pv cover) and showed decreasing trends in the minimum, maximum, and mean photosynthetic vegetation covers, with MK-stat values of -242, -134, and -190, respectively. The pv covers also showed negative Sen's slopes (Table 2) over the entire study period of -0.034, -0.156, and -0.091, respectively.

Table 2. Mann–Kendall and Sen's slope results for smoothed photosynthetic cover. We computed all statistics at 95% confidence (alpha = 0.05) [78,79].

Photosynthetic (Smoothed)	Mann-Kendall					Sen's Slope		
	Alpha	MK-Stat	z-Stat	*p*-Value	Trend	Alpha	Slope	Intercept
MEAN	0.05	−190	−3.945	0.00008	yes	0.05	−0.091	1.984
MAXIMUM	0.05	−134	−2.776	0.00550	yes	0.05	−0.156	3.669
MINIMUM	0.05	−242	−5.030	0.00000	yes	0.05	−0.034	0.718

The rasterized change detection results further support the statistical outcomes, showing a distinct decrease in photosynthetic fractional vegetative cover. Comparing the May 1990 image (Figure 2A) and the May 2019 image (Figure 2B) shows a distinct decrease in pv cover in the study area (Figure 6). Most pixels in the study area, and across Djibouti, decreased in pv between 1990 and 2019, while only small areas had increasing pv levels.
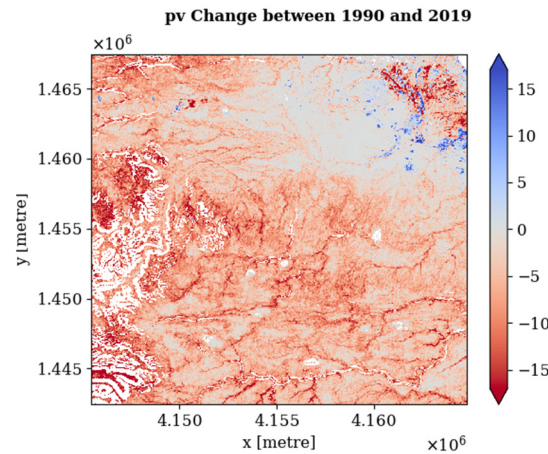
Figure 6. Change detection between 1990 pv and 2019 pv shows loss of pv in red, gain of pv in blue, and no change in grey. Most areas decreased in pv levels, while only small areas had increasing pv levels.

3.3. Zonal Summary Statistics

The pv and NDVI summary statistics over the 30-year study period (Figure 7) for the five districts of Djibouti (Figure 1C) show a positive relationship between pv and the NDVI. Ali Sabieh shows the greatest increase in pv between 1990 and 2005 (Figure 7C) and 2006 and 2020 (Figure 7D), and aligns with the NDVI results for the same region (Figure 7A,B). Dikhil and Tadjourah districts show maximum pv values at 100% in both the 1990–2005 (Figure 7C) and 2006–2020 (Figure 7D) periods. The statistical ranges for the Dikhil and Tadjourah districts were the greatest of all the districts for the full 30 years (showing the greatest variation in both pv and NDVI). Djibouti, Obock, and Tadjourah had the highest maximum NDVI values for both the 1990–2005 and 2006–20202 periods at 0.53, 0.59, and 0.65 (Figure 7A) and 0.61, 0.67, and 0.64 (Figure 7B), respectively.

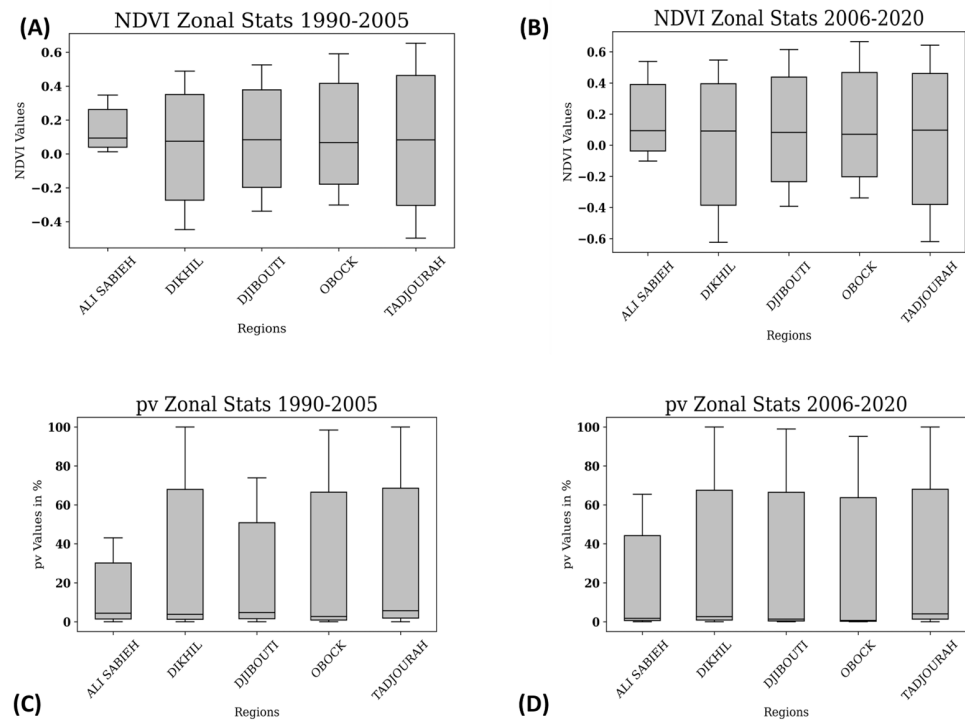**Figure 7.** NDVI and pv zonal statistics by region for 15-year periods. (**A**) NDVI statistics for 1990–2005 period. (**B**) NDVI statistics for 2006–2020 period. (**C**) pv statistics for 1990–2005 period. (**D**) pv statistics for 2006–2020 period.

4. Discussion

Here, we discuss the above rasterized results for a study area in SE Djibouti, the relationship between the FC and NDVI, and their general decreases over time. We also highlight the capabilities of DE Africa's ODC for processing and analyzing high volumes of satellite imagery and the results displaying decreasing trends in overall vegetation abundance and health. We discuss their implications toward heightened vulnerability in terms of agriculture and food production.

4.1. Temporal Vegetation Trends in Djibouti

The results suggest that throughout the study period, the Djibouti study area was covered by 35–60% of both non-photosynthetic vegetation and bare soil, and less than 10% of photosynthetic vegetation (Figure 5). The results also show a negative correlation between pv versus npv and bs [80]. This suggests the death of vegetation and the transition of those areas into bare soil, or the growth of vegetation into photosynthetic vegetation. Consequently, both the npv and bs covers demonstrated increasing trends over the study period as the pv cover decreased.

The district-level zonal statistics revealed a generally positive relationship between pv and the NDVI. The Tadjourah and Dikhil districts had the highest pv FC and NDVI (Figure 4) estimations, as well as the widest ranges throughout the study period. This suggests a greater presence of photosynthetic vegetation in these districts over a longer period, and a higher variability in the vegetation in Tadjourah and Dikhil. This finding spatially correlates with agricultural production in Djibouti being mostly concentrated in the more fertile land located primarily in the SE Djibouti study area and northwest regions (Figure 1C) of the country [81,82].

Focusing on the SE Djibouti study area (Figure 1C), a decreasing trend in total green vegetation was observed between 1990 and 2020 (Figure 2), with some periods of smaller positive trends from 1990 to 1995 and 1997 to 1999 and negative trends from 1995 to 1997 and 1999 to 2001. Between the years of 1997 and 2003, Djibouti underwent its most severe decline in pv over the study period.

Analyzing the change in photosynthetic (green) vegetation across all 119 scenes (Figure 5) revealed a clear decreasing trend when examining the and three-year moving averages (Figure 5A). The linear regression coefficient for the entire period from 1990 to 2020 indicated a consistent decline. However, the R-squared value was relatively low, indicating that the linear regression model did not fit the data well. To account for seasonal variability, we performed a yearly aggregation of the data (Figure 5B–D), which further accentuated the decreasing trend in green vegetation.

More specifically, the yearly smoothed minimum green fractional cover (Figure 5B), while exhibiting a slightly smaller regression, also confirmed the decreasing trend in the lowest pv values. The smoothed mean (Figure 5C) and maximum (Figure 5D) green fractional covers displayed decreasing trends as well, indicating that the average and highest levels of pv cover also decreased throughout the 30 years. These quantitative results aligned with the qualitative imagery observation of decreasing green fractional cover over the 30 years (Figure 2). The Mann–Kendall and Sen's slope statistical tests (Table 2) supported the rejection of the null hypothesis (of no change), indicating a significant decline in photosynthetic vegetation cover.

The raster results further substantiate the drastic change in photosynthetic fractional vegetative cover over the thirty years (Figure 7), and between the 10 May 1990 image (Figure 2A) and 10 May 2019 image (Figure 2B). These results demonstrate a distinct decrease in photosynthetic vegetation within the study area, highlighting the increasingly challenging environment in which plants grow and their inability to quickly adapt to a warming climate by relocating to new locales.

While there are minimal studies in the published literature using the NDVI and FC to specifically assess Djibouti's vegetative trends [83], the findings of this study align with the concerns about Djibouti published by the United Nations' Food and Agriculture

Organization [40] and Development Program [52], the World Bank [56], and the U.S. Agency for International Development's Famine Early Warning System [35], who all report on Djibouti's food insecurity and need to strengthen resiliency over the long term.

4.2. Connections between FC and NDVI

In other published works, the relationship between the FC and NDVI have been found to correlate positively with one another [69,84–88]. The general positive relationship between the FC and NDVI in this study and others is not surprising given that each is a measure of vegetation existence, abundance, and health. Carlson and Ripley (1997) [87] found the NDVI and fractional vegetation cover to be dependent, particularly when the NDVI is scaled between the limits of the minimum (bare soil) and maximum fractional vegetative cover [87]. Gao et al. (2020) reviewed algorithms for estimating the fractional cover using pure vegetation index values [69]. Their review of 173 selected scientific publications found that relative vegetation abundance (RA) algorithms for determining FC based on scaled maximum/minimum vegetation index values (such as the NDVI) are those most widely used, as opposed to other methods such as spectral mixture analysis (SMA), spectral-based supervised classification algorithms or machine learning algorithms [83]. They also noted that there were few regional studies of the fractional vegetative cover over Africa, Oceania and South/Central America presented in the reviewed literature [83].

The comparison between the FC and NDVI in these results offers valuable insights into their respective implications for assessing vegetation dynamics [69,84–87]. Firstly, the positive relationship observed between the FC and NDVI throughout the 30-year study period underscores their correlation. The peaks in the FC and NDVI in different years suggest temporal variations in vegetation health, with the FC peaking in one year and the NDVI in another. This implies that while both the FC and NDVI are related, they respond differently to changing environmental conditions or land management practices.

One notable finding is the maximum pv values at 100% observed in the Dikhil and Tadjourah districts in both the first and second halves of the study period. These districts also consistently exhibit the highest NDVI values, indicating a more robust photosynthetic vegetation cover than the other districts. This suggests that, in these districts, the FC and NDVI align closely [69,87,88], confirming the utility of both metrics in assessing vegetation health [69,87,88]. However, the variations in the range of NDVI values in these districts over the 30-year study period indicate the sensitivity of the NDVI to environmental changes that the FC may not fully capture [69].

The raster results further substantiate the correlation between the FC and NDVI. The distinct drop in green vegetative cover shown in the raster results between 1990 and 2019 (Figure 2) aligns with the quantified trends in the NDVI. This evidence reinforces the importance of FC as a valuable tool for monitoring and assessing changes in green vegetation cover, especially in under-studied regions like Djibouti [83], where such changes can have significant ecological, environmental, and socio-economic impacts [42,47,69,89,90].

4.3. Advantages of Data Processing in Datacubes

Utilizing DE Africa's ODC to access and analyze the study data resulted in a substantial reduction in both the processing time and the need for high-power computing resources.

Data cubes store spatial, spectral, and temporal data in multidimensional arrays [91] as opposed to traditional methods that involve downloading and maintaining individual images referenced as single files, requiring separate analysis steps for each file [15]. DE Africa's ODC provided analysis-ready data (ARD) and a processing platform for analysis and sharing [20] that saved time, effort and computing resources, allowing the analyst to spend more time on research and minimal time on data preparation and management [15,18,91,92]. Conducting the same study on a local PC, requiring the need to download, preprocess, and analyze data, would have taken an estimated 500% longer than the same study conducted on the DE Africa servers using the ODC. The parallel computing

of the DE Africa servers supports the complex workflows necessary for the sophisticated algorithms used in machine learning, image processing, and statistics [93].

4.4. Implications for Agriculture and Food Security

The results provide insights into the implications for agricultural vegetation in the 30-year period. Considering that agricultural vegetation is photosynthetic and that photosynthetic vegetation has declined over the study period, our results suggest that it has become more challenging to grow agricultural plant products in Djibouti. These results generally align with the findings of other researchers [9,94–96]. These implications are essential for understanding the dynamics and sustainability of agriculture and its larger implications for food security in Djibouti.

The negative trend of a mean pv of 0.00028% throughout the study period points to the loss of ~0.09 km^2 of arable land per year, and ~2.68 km^2 of arable land throughout the 30-year period between 1990 and 2020. Contrarily to the results of this study, the World Bank reports a 0.1% increase since 2000, and states that, in 2023, 0.15% of Djibouti's 23,200 km^2 was arable, which equates to 34.5 km^2 [50,56]. Considering these values, our study suggests that Djibouti loses about 0.2% of its arable land per year on average. Over the thirty-year period, Djibouti lost the equivalent of 7.7% of its currently arable land.

Unfortunately, in the absence of in situ data confirming the areas of true agricultural vegetation, it is difficult to precisely determine agricultural abundance and health over the study period. High-resolution remote sensing of the study area and hyperspectral imaging for the region are beyond the scope of this study but warrant further investigation to validate the results and confirm the agricultural trends independent of fractional cover. The trend toward decreasing photosynthetic vegetation is concerning enough to call for further investigations into why photosynthetic vegetation is decreasing, and possible mitigation strategies that could include increased political investments, adoption of climate-resilient farming styles, or increased planting of climate-resilient crops.

5. Conclusions

The major conclusion of this study is that, based on the FC and NDVI measures, Djibouti's vegetation has declined in abundance and health between the beginning of 1990 and the beginning of 2020. The ODC platform made processing quicker and easier than traditional GUI- or Python-based iterative methods. A lack of in situ data makes these conclusions less certain, but the comparison of FC and NDVI metrics suggests good agreement and provides supporting evidence for these further conclusions:

- The FC values for pv suggest an overall decline of vegetation abundance and health, in alignment with an increasingly arid environment and less photosynthetic vegetation, equating to a loss that is equivalent to ~7.7% of Djibouti's arable area.
- Districts with the greatest levels of pv and NDVI showed the greatest variability in those measures, pointing to the sensitive nature of photosynthetic vegetation in arid regions.
- Climate change, although not studied here, poses an imminent threat to photosynthetic vegetation, agriculture, and food security in Djibouti and other arid nations.

Overall, further investment in climate-resilient strategies would surely benefit Djibouti and the region, while improving geopolitical stability in the face of climate change and the connected challenges facing vegetation and agriculture in the Horn of Africa.

Conflicts of Interest: The authors declare no conflicts of interest.

References

1. Sun, W.Y.; Song, X.Y.; Mu, X.M.; Gao, P.; Wang, F.; Zhao, G.J. Spatiotemporal vegetation cover variations associated with climate change and ecological restoration in the Loess Plateau. *Agric. For. Meteorol.* **2015**, *209*, 87–99. [CrossRef]
2. Xu, X.K.; Chen, H.; Levy, J.K. Spatiotemporal vegetation cover variations in the Qinghai-Tibet Plateau under global climate change. *Chin. Sci. Bull.* **2008**, *53*, 915–922. [CrossRef]
3. Dore, M.H.I. Climate change and changes in global precipitation patterns: What do we know? *Environ. Int.* **2005**, *31*, 1167–1181. [CrossRef] [PubMed]
4. Huang, J.; Ji, M.; Xie, Y.; Wang, S.; He, Y.; Ran, J. Global semi-arid climate change over last 60 years. *Clim. Dyn.* **2016**, *46*, 1131–1150. [CrossRef]
5. El-Beltagy, A.; Madkour, M. Impact of climate change on arid lands agriculture. *Agric. Food Secur.* **2012**, *1*, 3. [CrossRef]
6. Aldababseh, A.; Temimi, M.; Maghelal, P.; Branch, O.; Wulfmeyer, V. Multi-Criteria Evaluation of Irrigated Agriculture Suitability to Achieve Food Security in an Arid Environment. *Sustainability* **2018**, *10*, 803. [CrossRef]
7. Rishmawi, K.; Prince, S.D.; Xue, Y. Vegetation Responses to Climate Variability in the Northern Arid to Sub-Humid Zones of Sub-Saharan Africa. *Remote Sens.* **2016**, *8*, 910. [CrossRef]
8. Grote, U.; Fasse, A.; Nguyen, T.T.; Erenstein, O. Food security and the dynamics of wheat and maize value chains in Africa and Asia. *Front. Sustain. Food Syst.* **2021**, *4*, 617009. [CrossRef]
9. Qu, C.; Hao, X. Agriculture drought and food security monitoring over the horn of Africa (HOA) from space. In Proceedings of the 2018 7th International Conference on Agro-geoinformatics (Agro-geoinformatics), Hangzhou, China, 6–9 August 2018; pp. 1–4.
10. USDA. *CropScape and Cropland Data Layers Information*; USDA: Washington, DC, USA, 2022.
11. Yin, H.; Brandão, A.; Buchner, J.; Helmers, D.; Iuliano, B.G.; Kimambo, N.E.; Lewińska, K.E.; Razenkova, E.; Rizayeva, A.; Rogova, N.; et al. Monitoring cropland abandonment with Landsat time series. *Remote Sens. Environ.* **2020**, *246*, 111873. [CrossRef]
12. Weier, J. *Measuring Vegetation (NDVI and EVI)*; Herring, D., Ed.; NASA: Washington, DC, USA, 2000.
13. Hazaymeh, K.; Hassan, Q.K. Remote sensing of agricultural drought monitoring: A state of art review. *AIMS Environ. Sci.* **2016**, *3*, 604–630. [CrossRef]
14. Bégué, A.; Madec, S.; Lemettais, L.; Leroux, L.; Interdonato, R.; Becker-Reshef, I.; Barker, B.; Justice, C.; Kerdilés, H.; Meroni, M. How well do EO-based food security warning systems for food security agree? Comparison of NDVI-based vegetation anomaly maps in West Africa. *IEEE J. Sel. Top. Appl. Earth Obs. Remote Sens.* **2023**, *16*, 1641–1653. [CrossRef]
15. Kopp, S.; Becker, P.; Doshi, A.; Wright, D.J.; Zhang, K.; Xu, H. Achieving the Full Vision of Earth Observation Data Cubes. *Data* **2019**, *4*, 94. [CrossRef]
16. ODC. Open Data Cube. Available online: https://www.opendatacube.org (accessed on 14 December 2022).
17. Wagner, W.; Bauer-Marschallinger, B.; Navacchi, C.; Reuß, F.; Cao, S.; Reimer, C.; Schramm, M.; Briese, C. A Sentinel-1 Backscatter Datacube for Global Land Monitoring Applications. *Remote Sens.* **2021**, *13*, 4622. [CrossRef]
18. ODC. Open Data Cube Overview. Available online: https://www.opendatacube.org/overview (accessed on 14 December 2022).
19. Wellington, M.J.; Renzullo, L.J.; Hosseini, M. High-Dimensional Satellite Image Compositing and Statistics for Enhanced Irrigated Crop Mapping. *Remote Sens.* **2021**, *13*, 1300. [CrossRef]
20. Africa, D. Digital Earth Africa. Available online: https://www.digitalearthafrica.org (accessed on 14 October 2022).
21. Digital Earth Africa. GeoMAD. 2022. Available online: https://docs.digitalearthafrica.org/en/latest/data_specs/GeoMAD_specs.html#Technical-information (accessed on 14 October 2022).
22. Digital Earth Africa. Fractional Cover. 2021 ed. 2021. Available online: https://docs.digitalearthafrica.org/en/latest/data_specs/Fractional_Cover_specs.html?highlight=fractional%20cover (accessed on 14 October 2022).
23. Govind, A. Towards Climate Change Preparedness in the MENA's Agricultural Sector. *Agronomy* **2022**, *12*, 279. [CrossRef]
24. Brown, M.E.; Funk, C.C.; Galu, G.; Choularton, R. Earlier famine warning possible using remote sensing and models. *Eos Trans. Am. Geophys. Union* **2007**, *88*, 381–382. [CrossRef]
25. Fre, Z.; Tsegay, B. Economic contribution of pastoral and agro pastoral production to food security and livelihoods systems in Africa: The case of Eastern Sudan, Eritrea and Western Ethiopia in the Horn of Africa. *Ethiop. E—J. Res. Innov. Foresight* **2013**, *5*, 14–31.
26. Oroda, A. Application of remote sensing to early warning for food security and environmental monitoring in the Horn of Africa. *Int. Arch. Photogramm. Remote Sens. Spat. Inf. Sci.* **2001**, *34*, W6.
27. Pavanello, S. Working across Borders—Harnessing the Potential of Cross-Border Activities to Improve Livelihood Security in the Horn of Africa Drylands. Oversees Development Institute-Humanitarian Policy Group. 2010. Available online: https://odi.org/en/publications/working-across-borders-harnessing-the-potential-of-cross-border-activities-to-improve-livelihood-security-in-the-horn-of-africa-drylands/ (accessed on 14 October 2022).
28. Sasson, A. Food security for Africa: An urgent global challenge. *Agric. Food Secur.* **2012**, *1*, 1–16. [CrossRef]
29. Thrupp, L.A.; Megateli, N. *Critical Links: Food Security and the Environment in the Greater Horn of Africa*; World Resources Institute: Washington, DC, USA, 1999.

30. Vogels, M.; de Jong, S.; Sterk, G.; Douma, H.; Addink, E. Spatio-Temporal Patterns of Smallholder Irrigated Agriculture in the Horn of Africa Using GEOBIA and Sentinel-2 Imagery. *Remote Sens.* **2019**, *11*, 143. [CrossRef]

31. Vrieling, A.; de Leeuw, J.; Said, M. Length of Growing Period over Africa: Variability and Trends from 30 Years of NDVI Time Series. *Remote Sens.* **2013**, *5*, 982–1000. [CrossRef]

32. UN. United Nations Global Issues Population. Available online: https://www.un.org/en/global-issues/population#:~:text=Africa:%20fastest%20growing%20continent,projected%20to%20double%20by%202050 (accessed on 14 December 2022).

33. Devereux, S.; Edwards, J. *Climate Change and Food Security*; John Wiley & Sons: Hoboken, NJ, USA, 2004.

34. Shiferaw, B.; Prasanna, B.M.; Hellin, J.; Bänziger, M. Crops that feed the world 6. Past successes and future challenges to the role played by maize in global food security. *Food Secur.* **2011**, *3*, 307–327. [CrossRef]

35. USAID. FEWS NET Djibouti Monitoring Report. Available online: https://fews.net/east-africa/djibouti (accessed on 12 December 2022).

36. United Nations. No. 46495. International Fund for Agricultural Development and Djibouti. In *United Nations Treaty Series*; UN: New York, NY, USA, 2018; 380p.

37. Magin, G. Djibouti. BirdLife International. 1999. Available online: http://www.datazone.birdlife.org/userfiles/file/IBAs/AfricaCntryPDFs/Djibouti.pdf (accessed on 15 September 2022).

38. Hassen, T.B.; El Bilali, H. Food security in the gulf cooperation council countries: Challenges and prospects. *J. Food Secur.* **2019**, *7*, 159–169. [CrossRef]

39. Mutopo, P.; Beyene, A.; Haaland, H.; Boamah, F.; Widengård, M.; Skarstein, R. *Biofuels, Land Grabbing and Food Security in Africa*; Bloomsbury Publishing: London, UK, 2011.

40. Food and Agricultural Organization of the United Nations. Djibouti Country Profile. Available online: https://www.fao.org/countryprofiles/index/en/?iso3=DJI (accessed on 14 October 2022).

41. Scarth, P.; Roder, A.; Schmidt, M. Tracking grazing pressure and climate interaction—The role of Landsat fractional cover in time series analysis. In Proceedings of the 15th Australasian Remote Sensing & Photogrammetry Conference (ARSPC), Alice Springs, Australia, 13–17 September 2010.

42. Hill, M.J.; Guerschman, J.P. Global trends in vegetation fractional cover: Hotspots for change in bare soil and non-photosynthetic vegetation. *Agric. Ecosyst. Environ.* **2022**, *324*, 107719. [CrossRef]

43. Ustin, S.L.; Roberts, D.A.; Gamon, J.A.; Asner, G.P.; Green, R.O. Using Imaging Spectroscopy to Study Ecosystem Processes and Properties. *BioScience* **2004**, *54*, 523–534. [CrossRef]

44. Dennison, P.; Roberts, D.A.; Chambers, J.Q.; Daughtry, C.S.; Guerschman, J.P.; Kokaly, R.F.; Okin, C.G.S.; Scarth, P.F. *Global Measurement of Non-Photosynthetic Vegetation*; NASA: Washington, DC, USA, 2016.

45. Liu, J.; Fan, J.; Yang, C.; Xu, F.; Zhang, X. Novel vegetation indices for estimating photosynthetic and non-photosynthetic fractional vegetation cover from Sentinel data. *Int. J. Appl. Earth Obs. Geoinf.* **2022**, *109*, 102793. [CrossRef]

46. Tian, J.; Su, S.; Tian, Q.; Zhan, W.; Xi, Y.; Wang, N. A novel spectral index for estimating fractional cover of non-photosynthetic vegetation using near-infrared bands of Sentinel satellite. *Int. J. Appl. Earth Obs. Geoinf.* **2021**, *101*, 102361. [CrossRef]

47. Guerschman, J.P.; Hill, M.J.; Renzullo, L.J.; Barrett, D.J.; Marks, A.S.; Botha, E.J. Estimating fractional cover of photosynthetic vegetation, non-photosynthetic vegetation and bare soil in the Australian tropical savanna region upscaling the EO-1 Hyperion and MODIS sensors. *Remote Sens. Environ.* **2009**, *113*, 928–945. [CrossRef]

48. Muir, J.; Schmidt, M.; Tindall, D.; Trevithick, R.; Scarth, P.; Stewart, J.B. *Field Measurement of Fractional Ground Cover*; Australian Bureau of Agricultural and Resource Economics and Sciences: Canberra, Australian, 2011.

49. Zheng, G.; Bao, A.; Li, X.; Jiang, L.; Chang, C.; Chen, T.; Gao, Z. The potential of multispectral vegetation indices feature space for quantitatively estimating the photosynthetic, non-photosynthetic vegetation and bare soil fractions in northern china. *Photogramm. Eng. Remote Sens.* **2019**, *85*, 65–76. [CrossRef]

50. World Bank. Djibouti. 2021. Available online: https://data.worldbank.org/country/djibouti (accessed on 22 September 2022).

51. CIA. *The World Factbook Country Summary*; CIA: Langley, VA, USA, 2022.

52. United Nations Development Programme. *Djibouti: Strengthening Resilience to Build Food Security*; United Nations Development Programme: New York, NY, USA, 2018.

53. United Nations Development Programme. *Djibouti*; United Nations Development Programme: New York, NY, USA, 2021.

54. United Nations Statistics. Djibouti Environment Statistics Country Snapshot. 2016. Available online: https://unstats.un.org/unsd/ENVIRONMENT/envpdf/Country_Snapshots_Dec_2016/Djibouti.pdf (accessed on 15 November 2022).

55. US Department of State. Djibouti. 2023. Available online: https://travel.state.gov/content/travel/en/international-travel/International-Travel-Country-Information-Pages/Djibouti.html (accessed on 14 October 2023).

56. World Bank. Djibouti. 2023. Available online: https://data.worldbank.org/country/djibouti (accessed on 14 September 2023).

57. United Nations Development Programme—Djibouti. 2023. Available online: https://www.dj.undp.org/ (accessed on 14 November 2023).

58. African Union. Djibouti. 2022. Available online: https://au.int/en/countryprofiles-3 (accessed on 30 March 2024).

59. World Health Organization. Djibouti. 2023. Available online: https://www.who.int/countries/dji/en/ (accessed on 15 November 2023).

60. United Nations Educational, Scientific and Cultural Organization. Djibouti. 2023. Available online: https://en.unesco.org/countries/djibouti (accessed on 14 November 2023).

61.   United Nations Conference on Trade and Development. *Djibouti: Harnessing Trade for Human Development in the Digital Age*; United Nations Conference on Trade and Development: Geneva, Switzerland, 2019.

62.   African Development Bank Group. Djibouti Economic Outlook. 2021. Available online: https://www.afdb.org/en/countries/east-africa/djibouti/djibouti-economic-outlook (accessed on 14 November 2022).

63.   Wardle, J.A.; Sagan, V.; Mohammed, F. Using Open Data Cube on the Cloud to Investigate Food Security by Means of Cropland Changes in Djibouti. *Int. Arch. Photogramm. Remote Sens. Spat. Inf. Sci.* **2022**, *XLIII-B3-2022*, 1039–1044. [CrossRef]

64.   Schmidt, M.; Denham, R.; Scarth, P. Fractional ground cover monitoring of pastures and agricultural areas in Queensland. In Proceedings of the 15th Australian Remote Sensing and Photogrammetry Conference (ARSPC), Alice Springs, Australia, 13–17 September 2010; pp. 13–17.

65.   Digital Earth Africa. Water Observations from Space. 2022. Available online: https://docs.digitalearthafrica.org/en/latest/data_specs/Landsat_WOfS_specs.html (accessed on 22 September 2022).

66.   National Aeronautics and Space Administration. Landsat 7 2021. Available online: https://landsat.gsfc.nasa.gov/satellites/landsat-7/ (accessed on 14 October 2022).

67.   Dask. Available online: https://docs.dask.org/en/stable/index.html (accessed on 22 February 2023).

68.   Jiang, Z.; Huete, A.R.; Chen, J.; Chen, Y.; Li, J.; Yan, G.; Zhang, X. Analysis of NDVI and scaled difference vegetation index retrievals of vegetation fraction. *Remote Sens. Environ.* **2006**, *101*, 366–378. [CrossRef]

69.   Gao, L.; Wang, X.; Johnson, B.A.; Tian, Q.; Wang, Y.; Verrelst, J.; Mu, X.; Gu, X. Remote sensing algorithms for estimation of fractional vegetation cover using pure vegetation index values: A review. *ISPRS J. Photogramm. Remote Sens.* **2020**, *159*, 364–377. [CrossRef] [PubMed]

70.   Elmore, A.J.; Mustard, J.F.; Manning, S.J.; Lobell, D.B. Quantifying vegetation change in semiarid environments: Precision and accuracy of spectral mixture analysis and the normalized difference vegetation index. *Remote Sens. Environ.* **2000**, *73*, 87–102. [CrossRef]

71.   Kendall, M.G. *Rank Correlation Methods*; Charles Griffin: London, UK, 1955.

72.   Kendall Tau Metric. 2023. Available online: https://encyclopediaofmath.org/index.php?title=Kendall_tau_metric (accessed on 22 September 2022).

73.   Sen, P.K. Estimates of the regression coefficient based on Kendall's tau. *J. Am. Stat. Assoc.* **1968**, *63*, 1379–1389. [CrossRef]

74.   Mann, H.B. Nonparametric tests against trend. *Econ. J. Econ. Soc.* **1945**, *13*, 245–259. [CrossRef]

75.   Daniel, W.W.; Cross, C.L. *Biostatistics: A Foundation for Analysis in the Health Sciences*; Wiley: Hoboken, NJ, USA, 2018.

76.   De Smith, M.J.; Goodchild, M.F.; Longley, P. *Geospatial Analysis: A Comprehensive Guide to Principles, Techniques and Software Tools*; Troubador Publishing Ltd.: Leicestershire, UK, 2007.

77.   Teegavarapu, R. *Trends and Changes in Hydroclimatic Variables: Links to Climate Variability and Change*; Elsevier: Amsterdam, The Netherlands, 2018.

78.   Hussain, e.a. pyMannKendall. Available online: https://pypi.org/project/pymannkendall/ (accessed on 18 May 2023).

79.   Hussain, e.a. pyMannKendall: A python package for non parametric Mann Kendall family of trend tests. *J. Open Source Softw.* **2019**, *4*, 1556. [CrossRef]

80.   Sutton, A.; Fisher, A.; Metternicht, G. Assessing the Accuracy of Landsat Vegetation Fractional Cover for Monitoring Australian Drylands. *Remote Sens.* **2022**, *14*, 6322. [CrossRef]

81.   Liu, W.; Chen, Y.; He, X.; Mao, P.; Tian, H. Is Current Research on How Climate Change Impacts Global Food Security Really Objective? *Foods* **2021**, *10*, 2342. [CrossRef]

82.   Muluneh, M.G. Impact of climate change on biodiversity and food security: A global perspective—A review article. *Agric. Food Secur.* **2021**, *10*, 1–25. [CrossRef]

83.   Gao, B.C. NDWI—A normalized difference water index for remote sensing of vegetation liquid water from space. *Remote Sens. Environ.* **1996**, *58*, 257–266. [CrossRef]

84.   Scanlon, T.M.; Albertson, J.D.; Caylor, K.K.; Williams, C.A. Determining land surface fractional cover from NDVI and rainfall time series for a savanna ecosystem. *Remote Sens. Environ.* **2002**, *82*, 376–388. [CrossRef]

85.   Jiménez-Muñoz, J.C.; Sobrino, J.A.; Plaza, A.; Guanter, L.; Moreno, J.; Martínez, P. Comparison between fractional vegetation cover retrievals from vegetation indices and spectral mixture analysis: Case study of PROBA/CHRIS data over an agricultural area. *Sensors* **2009**, *9*, 768–793. [CrossRef] [PubMed]

86.   Huang, S.; Tang, L.N.; Hupy, J.P.; Wang, Y.; Shao, G.F. A commentary review on the use of normalized difference vegetation index (NDVI) in the era of popular remote sensing. *J. For. Res.* **2021**, *32*, 1–6. [CrossRef]

87.   Carlson, T.N.; Ripley, D.A. On the relation between NDVI, fractional vegetation cover, and leaf area index. *Remote Sens. Environ.* **1997**, *62*, 241–252. [CrossRef]

88.   Carlson, T.N.; Gillies, R.R.; Perry, E.M. A method to make use of thermal infrared temperature and NDVI measurements to infer surface soil water content and fractional vegetation cover. *Remote Sens. Rev.* **1994**, *9*, 161–173. [CrossRef]

89.   Xiao, J.; Moody, A. A comparison of methods for estimating fractional green vegetation cover within a desert-to-upland transition zone in central New Mexico, USA. *Remote Sens. Environ.* **2005**, *98*, 237–250. [CrossRef]

90.   Guan, K.; Wood, E.F.; Caylor, K. Multi-sensor derivation of regional vegetation fractional cover in Africa. *Remote Sens. Environ.* **2012**, *124*, 653–665. [CrossRef]

91. Appel, M.; Pebesma, E. On-Demand Processing of Data Cubes from Satellite Image Collections with the gdalcubes Library. *Data* **2019**, *4*, 92. [CrossRef]

92. Killough, B.; Siqueira, A.; Dyke, G. Advancements in the Open Data Cube and Analysis Ready Data—Past, Present and Future. In Proceedings of the IGARSS 2020—2020 IEEE International Geoscience and Remote Sensing Symposium, 26 September–2 October 2020; pp. 3373–3375.

93. Anaconda. Dask Distributed Documentation. Available online: https://distributed.dask.org/en/latest/ (accessed on 13 September 2023).

94. Zhou, J.; Chen, J.; Chen, X.; Zhu, X.; Qiu, Y.; Song, H.; Rao, Y.; Zhang, C.; Cao, X.; Cui, X. Sensitivity of six typical spatiotemporal fusion methods to different influential factors: A comparative study for a normalized difference vegetation index time series reconstruction. *Remote Sens. Environ.* **2021**, *252*, 112130. [CrossRef]

95. African Union, Semi-Arid Food Grain Research and Development. Challenges and Opportunities for Strategic Agricultural Commodity Value Chains Development in the IGAD Region. 2014. Available online: https://archives.au.int/bitstream/handle/ 123456789/1973/Challenges%20and%20Opportunities%20for%20Strategic%20Agricultural%20Commodity%20Value%20 Chains_E.pdf?sequence=1&isAllowed=y (accessed on 22 September 2022).

96. Chandrasekharam, D.; Lashin, A.; Nassir Al, A.; Al-Bassam, A.M.; Varun, C. Geothermal energy for desalination to secure food security: Case study in Djibouti. *Energy Sustain. Soc.* **2019**, *9*, 24. [CrossRef]